Neuroscience Vol. 51, No. 1, pp. 55–64, 1992
Printed in Great Britain

0306-4522/92 $5.00 + 0.00
Pergamon Press Ltd

REGULATION OF TRANSIENT DOPAMINE CONCENTRATION GRADIENTS IN THE MICROENVIRONMENT SURROUNDING NERVE TERMINALS IN THE RAT STRIATUM

K. T. KAWAGOE, P. A. GARRIS, D. J. WIEDEMANN and R. M. WIGHTMAN*

Department of Chemistry and Curriculum In Neurobiology, CB # 3290, Venable Hall, University of North Carolina at Chapel Hill, Chapel Hill, NC 27599-3290, U.S.A.

Abstract—Synaptic overflow of dopamine in the striatum has been investigated during electrical stimulation of the medial forebrain bundle in anesthetized rats. Dopamine has been detected with Nafion-coated, carbon-fiber electrodes used with fast-scan voltammetry. In accordance with previous results, dopamine synaptic overflow is a function of the stimulation frequency and the anatomical position of the carbon-fiber electrode. In some positions the concentration of dopamine is found to respond instantaneously to the stimulus when the time-delay for diffusion through the Nafion film is accounted for. In these locations the measured rates of change of dopamine are sufficiently rapid such that extracellular diffusion is not apparent. The rate of dopamine overflow can be described by a model in which each stimulus pulse causes instantaneous release, and cellular uptake decreases the concentration between stimulus pulses. Uptake is found to be described by a constant set of Michaelis–Menten kinetics at each location for concentrations of dopamine from 100 nM to 15 μM. The concentration of dopamine released per stimulus pulse is found to be greatest at low frequency ($\leq$ 10 Hz) with stimulus trains, and with single-pulse stimulations in nomifensine-treated animals. The frequency dependence of release is not an effect of dopamine receptor activation; haloperidol (2.5 mg/kg) causes a uniform increase in release at all frequencies.

The absence of diffusional effects in the measurement locations means that the constants determined with the electrode are those operant inside intact striatal tissue during stimulated overflow. These values are then extrapolated to the case where a single neuron fires alone. The extrapolation shows that while the transient concentration of dopamine may be high (200 nM) at the interface of the synapse and the extrasynaptic region, it is normally very low ($<$ 6 nM) in the bulk of extracellular fluid.

An understanding of the factors which influence dopamine concentration in the extracellular fluid is important to discern the role of dopamine in neurotransmission. If appreciable concentrations of dopamine exist only in synaptic regions, then dopamine acts as a classical transmitter. Alternatively, if dopamine released from one terminal reaches concentrations in the extrasynaptic region that are sufficiently high to activate receptors over a wide spatial range, it may act as a neuromodulator.[34] The concentration of dopamine in the extracellular fluid of the rat brain has been the subject of several investigations,[4,14,42,54] and current estimates range from 5 to 50 nM. Extracellular concentrations in these ranges have been demonstrated to affect postsynaptic neurons in the striatum with the combined use of electrophysiology and *in vivo* voltammetry.[52,53]

The synaptic concentration of dopamine is a function of the balance of release from terminals, cellular uptake, and metabolism,[17] although the latter process operates on a significantly longer time-scale.[12] Since release and uptake are rapid events, dopamine which leaves the synapse will generate a transient concentration gradient controlled by extracellular diffusion. Thus, to understand the transient regulation of dopamine the central issues are release, uptake, and diffusion. Many techniques such as *in vivo* dialysis sample the spatially and temporally averaged extracellular concentration.[4,37] However, a much different picture may emerge if viewed in real time at the outer edge of a synapse. Fast-scan cyclic voltammetry[25,32] provides the temporal resolution to aid in such a view.

In previous work we have examined the rates of dopamine release, uptake and diffusion from synaptic overflow measurements made with carbon-fiber electrodes in the caudate nucleus during stimulation of the ascending dopaminergic fibers.[49] The stimulation is designed so that the neurons are forced to fire in synchrony for a short interval ($<$ 5 s). The concentration of dopamine measured during stimulated synaptic overflow varies with electrode location[29,44,52] and is a function of the frequency and duration of the stimulus train.[14,24] After stimulation, the dopamine rapidly disappears from the extracellular space as a result of cellular uptake, and can be described by Michaelis–Menten kinetics. Based on the assumptions that each stimulus pulse releases an instantaneous concentration from a group of neurons

*To whom correspondence should be addressed.

adjacent to the electrode and that uptake between pulses follows Michaelis–Menten kinetics, we have shown that the transient concentration changes can be described with a single set of parameters over a wide range of stimulus frequencies.[51] If release, uptake, and diffusion are appropriately accounted for, the model should allow extrapolation to overflow concentrations in the unstimulated animal.

In previous papers we have refrained from assigning any fundamental meaning to the values of the parameters because of their interdependence; i.e. misassignment of one value would alter the values of the others. It is particularly difficult to model dopamine diffusion in the brain when uptake is simultaneously occurring.[34] However, in certain areas of the striatum we will show that diffusion measured in synaptic overflow experiments is negligible in the extracellular space. In these locations, release and uptake can readily be evaluated. When the dynamics of release and uptake of stimulated synaptic overflow of dopamine are explored under these conditions at frequencies close to physiological firing rates, data are obtained which can be extrapolated to the unstimulated animal.

EXPERIMENTAL PROCEDURES

Surgical procedures

Male Sprague–Dawley rats (300–400 g, Charles River Laboratories, Wilmington, MA) were anesthetized with urethane (1.5 g/kg), placed in a stereotaxic frame, and maintained at 37°C. A carbon-fiber working electrode was lowered into the caudate nucleus (1.2 mm AP, 2.0 mm ML, 4.5 mm DV of bregma) and a bipolar stimulating electrode (Plastics Products, Roanoke, VA) was positioned in the medial forebrain bundle (− 4.5 mm AP, 1.6 mm ML, 8.5 mm DV) as described previously.[30] The working electrode position was vertically moved to obtain maximum overflow.[29]

Electrical stimulation

The electrical stimulation trains were computer-generated and consisted of 350 μA constant current, biphasic pulses (2 ms/phase) at stimulation frequencies from 10 to 60 Hz. Usually the pulse trains consisted of 120 pulses, and the time between stimulations was 7 min. The order in which the frequencies were tested was random. For the measurement of overflow from single stimulation pulses, 20–60 stimulations repeated at 45-s intervals were averaged together.

Post mortem *tissue analysis*

The tissue content of dopamine was determined by liquid chromatography with electrochemical detection following decapitation and dissection of the caudate.[24] For comparison with *in vivo* data, animals were anesthetized with 1.5 g/kg urethane and killed 2 h after anesthesia. Rats receiving haloperidol (2.5 mg/kg) were killed 20 min after drug administration.

Electrochemistry

Carbon-fiber (10 μm) working electrodes were prepared with an elliptical tip.[19] The electrodes were coated with Nafion by dip-coating in an isopropanol solution containing 2.5% Nafion. This is a more dilute concentration than used in previous work,[30] and results in electrodes with faster response times to changes in dopamine concentration.

Fast-scan (300 V/s) cyclic voltammetry was employed with a potentiostat (EI-400, Ensman Instrumentation, Bloomington, IN) that was computer-controlled.[48] Scans were repeated at 100-ms intervals, and the current at the oxidation potential for dopamine was obtained from successive voltammograms and scaled to concentration with calibration curves obtained after the *in vivo* experiment. Calibration curves are linear over the range of dopamine concentrations observed *in vivo*.[47] Overflow curves recorded at a single electrode position in the striatum were averaged to improve signal-to-noise ratios.

Data analysis

Calibration factors and the diffusional delay caused by the Nafion film for each electrode was measured by postcalibration. The electrode was exposed to a square-wave concentration profile of dopamine of known concentration with a flow-injection apparatus.[23] The effects of diffusion were deconvoluted via the Fourier transform method[2,39] from the *in vivo* overflow curves (see Appendix).

The rates of release and uptake of dopamine were obtained from the deconvoluted data. The rate of uptake (-d[DA]/dt) after stimulation was fitted to Michaelis–Menten kinetics:

$$-\mathrm{d[DA]}/\mathrm{d}t = V_{max}/\{(K_m/[\mathrm{DA}]) + 1\}, \qquad (1)$$

where [DA] is the instantaneous concentration of dopamine. The value of K_m was taken to be 0.16 μM.[33] The value of V_{max} was measured from the descending slope after a 5-s, 60-Hz stimulation, a condition which results in a concentration of dopamine sufficiently large that uptake is saturated ([DA] > K_m). During stimulation, the rate of appearance of dopamine (d[DA]/dt was assumed to follow[51]

$$\mathrm{d[DA]}/\mathrm{d}t = (f)[\mathrm{DA}]_p - (V_{max}/\{(K_m/[\mathrm{DA}]) + 1\}), \quad (2)$$

where f is the stimulation frequency (Hz) and $[\mathrm{DA}]_p$ is the concentration change of dopamine per stimulus pulse. At low stimulation frequencies overflow becomes steady-state and, thus, $[\mathrm{DA}]_p = (1/f)\ V_{max}/((K_m/[\mathrm{DA}]) + 1)$.[49] In previous work, a single

value of $[DA]_p$ was used to simulate all frequencies.[49] Here, the value of $[DA]_p$ was determined from synaptic overflow curves at each frequency. The determined constants were used to simulate overflow curves with the integrated forms of Equations 1 and 2. These were convoluted with diffusion through Nafion and compared with the measured response. The coefficient of determination, r^2, was used as an index of the goodness of fit of the model to the data.

Values are reported as the average ± S.E.M. Tukey's test for *post hoc* pair-wise comparisons was made when justified by analysis of variance. Statistics were computed using Systat (SYSTAT, Inc., Evanston, IL).

Reagents and drugs

Drugs were administered intraperitoneally Nomifensine Maleate (Hoechst Roussel Pharmaceuticals Inc., Somerville, NJ) and haloperidol (Sigma Chemical Corp., St Louis, MO) were administered in physiological saline with tartaric acid (pH 4–6 adjusted with NaOH).

RESULTS

Heterogeneity of dopamine overflow

Concentration–time profiles measured in the caudate nucleus during 2-s, 60-Hz stimulations of the medial forebrain bundle are shown in Fig. 1 for four different ventral positions of the working electrode separated by 100 μm in the same animal. A background-subtracted voltammogram is also shown in Fig. 1, which verifies that dopamine is the species detected *in vivo*. At each electrode position the peak concentration of dopamine, the time-delay between the termination of the stimulus and the maximal concentration, and the rates of appearance and disappearance of dopamine are all different. While heterogeneity of the concentration of stimulated overflow has previously been reported,[29,44,52] the variation in the delay of dopamine to reach its maximum after stimulation has not. At a depth of 4.9 mm the delay is 0.2 s (Fig. 1). The delay increases to 2 s at 5.0 mm and decreases with further lowering while the concentration elicited from the stimulation approximately triples.

The response time of the electrode was evaluated after *in vivo* use, and the time-lag from diffusion through the Nafion film was removed from the central, lower panel of Fig. 1 by deconvolution using the procedure described in the Appendix. The result shown in the lower right panel of Fig. 1 differs considerably from the originally recorded signal. The overflow ceases with termination of the stimulation, and the rates of appearance and disappearance are greater. When each response in Fig. 1 is deconvoluted, the delays at 4.9 and 5.2 mm are completely removed, however, some delay remains at both 5.0 mm (0.9 s) and 5.1 mm (0.2 s).

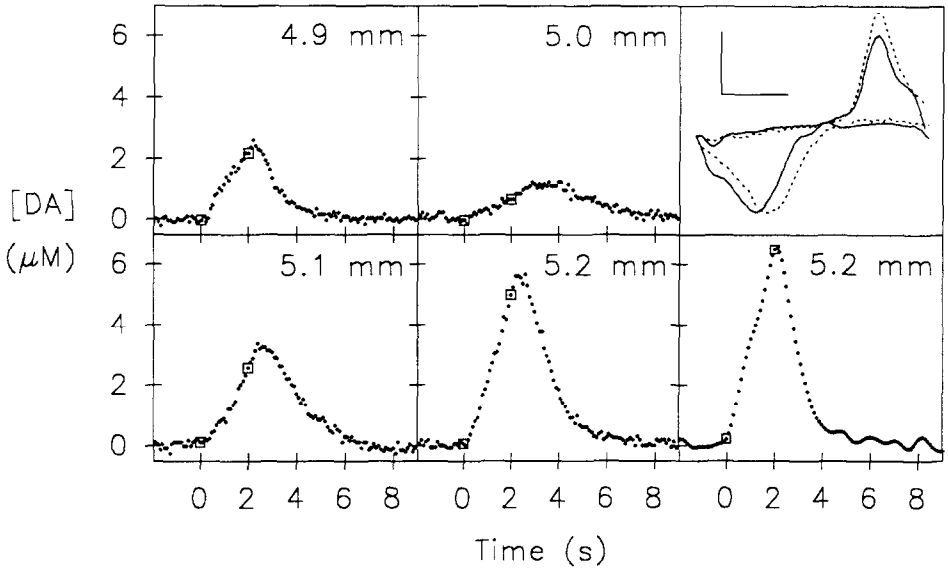

Fig. 1 Heterogeneity of dopamine overflow in a single rat striatum. Overflow curves were measured during a 2-s, 60-Hz electrical stimulation of the media forebrain bundle at different ventral working electrode positions. The top right panel shows the background-substracted, cyclic voltammogram collected *in vivo* at a depth of −5.2 mm (—). The vertical calibration bar is 0.3 nA and the horizontal scale bar is 0.4 V. The overlaid voltammogram (- - -) was obtained for dopamine *in vitro*. In the remaining panels the concentration of dopamine obtained from the peak oxidative current in successive voltammograms is shown, and the depth from dura of the electrode tip is indicated. The initiation and the termination of the stimulation pulses is indicated by the open squares at zero and two seconds, respectively. The bottom right panel is the same data as the bottom central panel after deconvolution of the contribution of diffusion through the Nafion film. The film thickness calculated from the postcalibration response is 365 nm.

In each animal in this study the working electrode position was adjusted as demonstrated in Fig. 1 to obtain relatively large concentrations of dopamine overflow with a small delay between the end of the stimulation pulses and the peak dopamine response. Deconvolution of the time-delay caused by diffusion through the Nafion film in these locations always eliminates the time-delay between termination of the stimulation and the descent of the dopamine concentration.

Frequency response of overflow

The change in concentration induced by a 10-Hz stimulation differs from that obtained with 60-Hz (Fig. 2). During the 10-Hz stimulation, the dopamine concentration increases when the stimulation is initiated, reaches a steady state, and returns to base line levels when the stimulation is terminated. In contrast, the dopamine concentration increases during the entire 60-Hz stimulation interval. The same uptake parameters (V_{max} and K_m) can be used to simulate the disappearance after stimulation for each curve when diffusion through the Nafion is accounted for (solid lines, Fig. 2). However, the value of $[DA]_p$ required to simulate synaptic overflow obtained during 10-Hz stimulations is twice as large as that used to model the 60-Hz response in this animal. When overflow curves from many animals were simulated, it was found that this was universally the case (Fig. 3). Values of $[DA]_p$ required to obtain a good simulation are independent of frequency with 20–60-Hz stimulations and had a mean value of 87 ± 7 nM ($n = 12$), but the values of $[DA]_p$ at 10-Hz are twice as large (Fig. 4).

Effect of haloperidol on synaptic overflow

To examine whether the frequency dependence of $[DA]_p$ is caused by interactions with dopamine receptors, overflow was examined after administration of 2.5 mg/kg haloperidol. This large dose

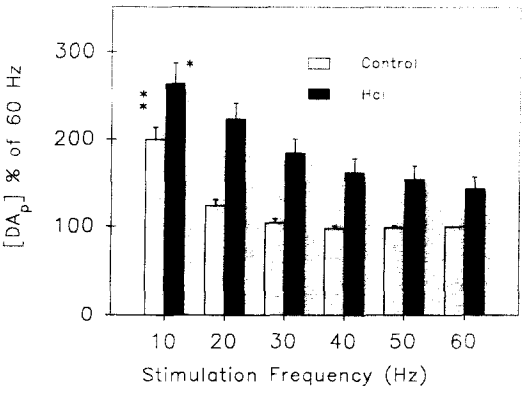

Fig. 3. $[DA]_p$ values obtained at different stimulation frequencies normalized to values obtained from 60-Hz stimulations. The groups include animals treated with anesthetic [Control, treated with 1.5 g/kg urethane ($n = 18$ animals)] and anesthetic + haloperidol [Hal, 2.5 mg/kg ($n = 6$ animals)]. For haloperidol-treated animals, data are normalized to $[DA]_p$ determined from data obtained prior to drug administration. **Different from control group values for stimulation frequencies from 20 to 60-Hz, $P \leq 0.001$; *different from haloperidol group values for stimulation frequencies from 30 to 60-Hz, $P \leq 0.05$.

of the dopamine receptor antagonist was used to attenuate autoinhibition of synaptic overflow.[47] Haloperidol caused a significant increase in $[DA]_p$ at all frequencies ($166 \pm 6\%$ of predrug response, $n = 6$ animals), but the value of $[DA]_p$ at 10-Hz was still higher than at other frequencies (Fig. 3). Haloperidol did not alter the tissue content of dopamine [60.5 ± 3.2 nmol/g ($n = 4$) compared with 57.5 ± 4.3 nmol/g ($n = 4$) in control animals].

Overflow of dopamine with a single pulse after nomifensine

In animals in which uptake of dopamine is inhibited with nomifensine, overflow from a single-stimulation pulse can be measured *in vivo*.[25] Nomifensine causes an increase in overflow by increasing the

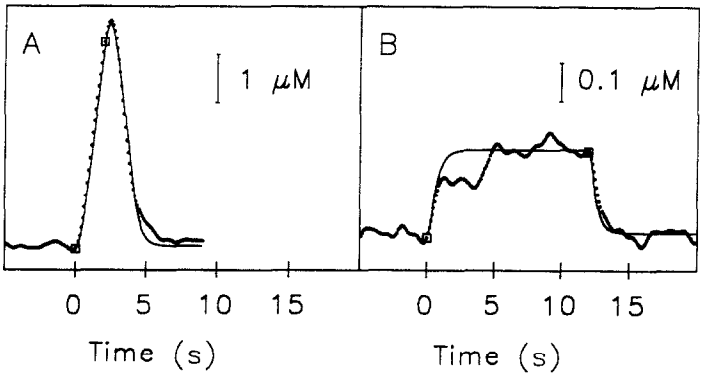

Fig. 2. Dopamine overflow in the caudate nucleus of a single animal during 10- and 60-Hz, 120-pulse stimulations of the medial forebrain bundle (• • •) and simulated (——) responses. The open squares indicated the initiation and termination of the stimulus train. (A) Overflow measured during a 2-s, 60-Hz stimulation. Simulation parameters: $[DA]_p = 80$ nM, $V_{max} = 2.78$ μM, $K_m = 0.16$, and Nafion film thickness of 325 nm. $r^2 = 0.99$. (B) The overflow measured during a 12-s, 10-Hz stimulation. Simulation parameters were the same except $[DA]_p = 160$ nM. $r^2 = 0.88$.

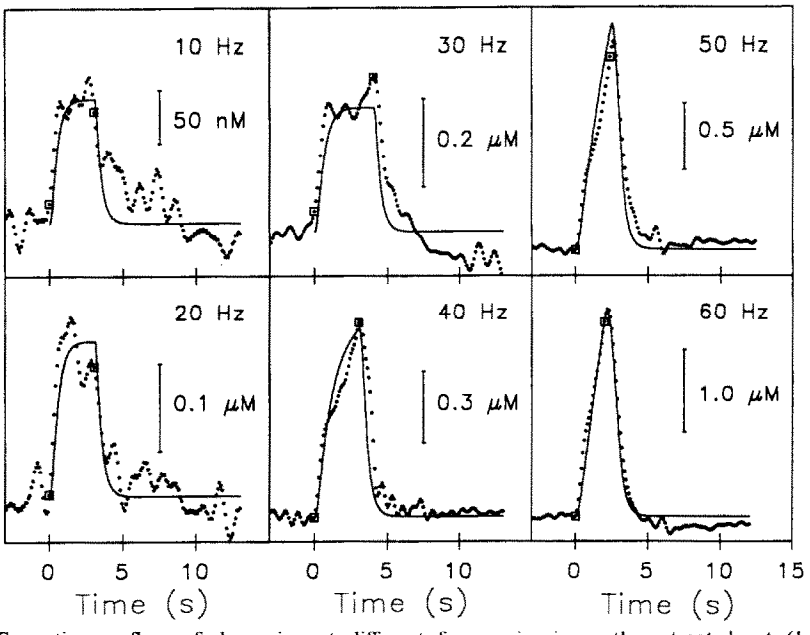

Fig. 4. Synaptic overflow of dopamine at different frequencies in urethane-treated rat (1.5 g/kg). The open squares indicate the initiation and termination of a stimulus train. Stimulation frequencies are indicated in each panel. Overflow curves from 30- 60-Hz stimulations were fitted using the simplex method[39] for the determination $[DA]_p$ and V_{max}. Simulations, shown by the solid lines, employed the following parameters: Nafion film thickness 300 nm, $V_{max} = 3.56\,\mu M/s$, and $K_m = 0.16\,\mu M$. The value of $[DA]_p$ was 75 nM for all frequencies except 20-Hz (93 nM) and 10-Hz (150 nM).

apparent value of K_m for uptake.[28] Overflow after a single-pulse stimulation in an animal treated with nomifensine (25 mg/kg) is seen as an increase in dopamine concentration which occurs over approximately 1 s followed by a return to prestimulus levels (Fig. 5). Deconvolution of the electrode response shows that the increase in dopamine concentration occurs within the first 100 ms after the stimulation.

The instantaneous rise in dopamine as a result of a single-stimulus pulse is a direct measure of $[DA]_p$ with an average value of 260 ± 70 nM ($n = 7$ animals). In contrast the value of $[DA]_p$ measured in these animals from dopamine overflow curves during high-frequency pulse trains was 120 ± 20 nM. The exponential decay reflects dopamine uptake under unsaturated conditions. The exponential rate-constant, which should correspond to V_{max}/K_m, was 0.9 ± 0.2/s in animals treated with 25 mg/kg nomifensine. V_{max} (obtained after high-frequency stimulations) was $2.86 \pm 0.63\,\mu M/s$. The apparent K_m after nomifensine, determined from the rate of disappearance after 120 pulse stimulations at frequencies from 10 to 60 Hz, was $3.6 \pm 1.4\,\mu M$ ($n = 7$). Their ratio ($V_{max}/K_m = 1.3 \pm 0.2$/s) is in reasonable agreement with that obtained in the same animals with single-pulse stimulations.

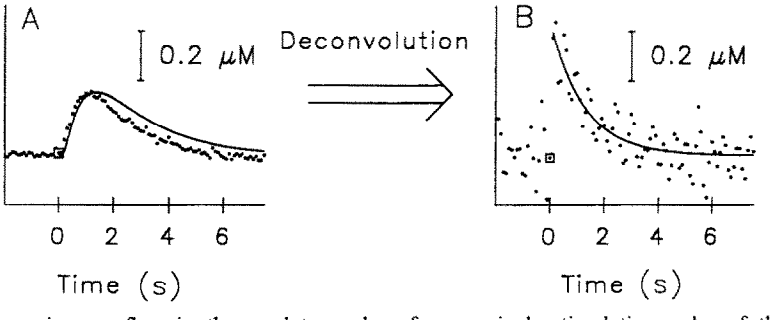

Fig. 5. Dopamine overflow in the caudate nucleus from a single stimulation pulse of the medial forebrain bundle in animals treated with nomifensine (25 mg/kg). (A) Overflow (20 single stimulation pulses averaged) measured in one animal (• • •) and simulation (——). Simulation parameters: $V_{max} = 4.38\,\mu M$, $[DA]_p = 0.45\,\mu M$, $K_m = 8.48\,\mu M$, and Nafion thickness of 420 nm. $r^2 = 0.80$. (B) Deconvoluted overflow (• • •) and equivalent simulated response (——). Rate constant 0.79/s. $r^2 = 0.73$.

DISCUSSION

Concentration gradients during stimulated synaptic overflow in the striatum

Spatial heterogeneity of dopamine overflow (Fig. 1) is a prominent feature of stimulated overflow measurements made with carbon-fiber electrodes in the caudate nucleus.[29,44,52] Heterogeneity within the rat striatum has also been reported using autoradiographic techniques.[7,43,46] In this work heterogeneity was observed both in concentration during overflow and in the time-delay for dopamine to begin its decrease in concentration after stimulation. In all of the experiments reported here, the electrode position was adjusted so that the time-delay was minimal.

In these locations, the time-delay for the onset of dopamine disappearance can be accounted for by diffusion of dopamine through the Nafion film. Nafion is a polymeric, cation-exchange material that is used on the electrode tip to provide chemical selectivity and to prevent protein fouling of the electrode surface.[22] While these features are advantageous for *in vivo* measurements of dopamine, Nafion impedes the diffusion of dopamine to the electrode surface, and complicates the evaluation of diffusion of dopamine in the extracellular space. Deconvolution of this process results in overflow curves which immediately descend when the stimulation is terminated. Unit activity of dopamine cell bodies actually diminishes below basal firing rates at the end of medial forebrain bundle stimulations,[26] and release would be expected to cease as well. Thus, the deconvoluted data provide a view expected for release and uptake occurring adjacent to the electrode.

If release or uptake occur at a site remote from the electrode, an additional time-delay caused by diffusion through brain tissue would be expected. Since the time resolution of the deconvoluted data is 100 ms, the maximal diffusional distance can be calculated to be less than 8 μm assuming a diffusion coefficient of 6×10^{-6} cm^2/s in the extracellular fluid. Thus, diffusion in the extracellular fluid plays a minor role in these locations in the striatum, and the rates of release and uptake can be characterized.

Concentration gradients exist over distances of 100 μm, as shown in Fig. 1. However, the events observed *in vivo* are so rapid that they only reflect concentrations directly adjacent to the electrode.[11] The density of dopaminergic terminals in the striatum[7] has been determined to be approximately 1×10^8/mm^3. Thus, on the time-scale of our measurements it is unlikely that there is a concentration gradient between adjacent nerve terminals during stimulations which force all terminals to release simultaneously. Therefore, the concentration in the extracellular fluid surrounding the nerve terminals is uniform. The calculated concentration gradients for a pulsed concentration step equilibrates in 100–200 ms over an 8-μm distance, as shown in Fig. 6. As shown in our previous work, the electrode is at least this close to the secreting terminals.[1] Thus, the small distance between the release sites during stimulated synaptic overflow and the detecting electrode means that the concentration detected at the electrode is close to that adjacent to the release sites.* The concentrations observed with the electrode at these locations must be equivalent to those which occur at the *interface* between the synapse and the extrasynaptic region.

The concentration changes which occur inside the synapse are likely to be very different from those observed in these measurements.[9] As pointed out by del Castillo and Katz[6] the concentration of neurotransmitter observed at extrasynaptic locations will be diluted from the actual synaptic concentration. The majority of dopaminergic synapses in the dorsolateral striatum are of small diameter (0.15–0.39 μm) with a cleft of approximately 0.02 μm.[38] The synaptic region appears to contain the preponderance of uptake sites for dopamine since these are found in greatest abundance in the P2 fraction[33] of brain homogenates, the fraction which contains the releasable stores of dopamine.[21] Transient, large micromolar-concentration spikes may occur in the synapses as seen at the surface of cultured adrenal medullary cells during stimulated exocytosis.[50] Co-localization of uptake and release sites in the synapse would lead to large concentration

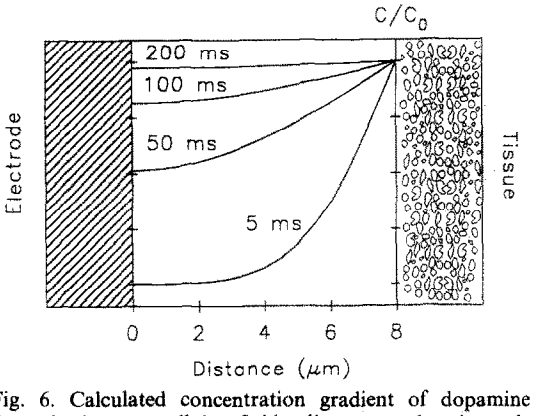

Fig. 6. Calculated concentration gradient of dopamine through the extracellular fluid adjacent to the electrode surface during conditions of stimulated overflow. The spatially dependent concentration (C) is normalized to the source concentration (C_0), which is assumed to be uniform in the tissue. Individual lines represent the concentration gradient between the source and the electrode surface at fixed time intervals. At 0.2 s, the surface electrode concentration is 97% of the source concentration. Concentration profiles were calculated from analytical expression for diffusion though a thin sheet (Equation 4.17 in Ref. 5). Simulation parameters: $D = 6 \times 10^{-6}$ cm^2/s, diffusion distance 8 μm.

*Fast-scan cyclic voltammetry generates a concentration gradient which is spatially restricted within the Nafion film.[22]

gradients inside the cleft. The quantal nature of exocytosis dictates that this will be the case.[18] However, the interfacial synaptic–extracellular fluid concentration is expected to be the same as the time-averaged synaptic concentration.[9]

Kinetic characterization of stimulated synaptic overflow of dopamine in the striatum

When diffusion is negligible or appropriately accounted for, the measured overflow curves provide information of the rates of uptake and release. As shown, the data fit well to a simple model[51] for these processes. The model makes two central assumptions concerning dopamine uptake: (i) uptake obeys Michaelis–Menten kinetics with a single, high-affinity uptake site; and (ii) temporally, dopamine uptake is a continuous process, i.e. dopamine uptake occurs between stimulation pulses. The validity of the first assumption is demonstrated by comparing overflow curves with the simulations. The extracellular clearance of dopamine after cessation of the stimulus is well described by the model over a wide concentration range from 100 nM (observed after a 3-s, 10-Hz stimulation) to 15 μM (observed after a 5-s, 60-Hz stimulation) and after a single stimulus pulse. The presence of a low-affinity, high capacity uptake site[44] can not entirely be ruled out. This putative uptake site would decrease the evoked overflow observed at high concentrations and lead to an underestimation of $[DA]_p$. However, the model fits the recorded overflow curves at high dopamine concentrations remarkably well.

The validity of the second assumption that dopamine uptake immediately follows release is best demonstrated by examining single-pulse stimulations. When the response time for dopamine to traverse the Nafion film at the tip of the electrode is removed by deconvolution, the maximal increase in dopamine concentration in nomifensine-treated animals is seen to increase almost immediately after the stimulation pulse and then decay in an exponential fashion. Since the concentration released is much lower than the apparent value of K_m in nomifensine-treated animals, uptake of dopamine following a single-pulse stimulation functions under nonsaturated conditions. Thus, the deconvoluted response to a one-pulse stimulation confirms that uptake occurs immediately after a stimulus pulse. The immediate increase in dopamine concentration in this experiment provides a direct measure of $[DA]_p$. Since the cell body is depolarized within milliseconds by each pulse[26] an instantaneous response would also be expected from the nerve terminals. This maximal response is a direct measurement of $[DA]_p$, and was 2.5-times greater than found during high-frequency stimulus trains.

The presence of Michaelis–Menten uptake kinetics has important implications for the determination of release from synaptic overflow curves. An estimate of release by the division of the maximum concentration elicited at each frequency by the number of pulses in the stimulus train is altogether inappropriate since the rate of uptake is dependent on substrate concentration during unsaturated conditions. However, this approach has been used to estimate norepinephrine release in the paraventricular nucleus of the hypothalamus *in vivo* with the conclusion that release increases with frequency[45] which is in sharp contrast to the findings reported here and in *in vitro* studies.[16,20,31] This discrepancy could well be explained by the failure to properly account for uptake in determining release. The simple calculation of release is only appropriate when uptake is constant, i.e. non-Michaelis–Menten, or very low. The release of vasopressin *in vitro* from the neural lobe of the pituitary has correctly been calculated in this manner because uptake does not play a significant role in peptidergic neurons and, in fact, vasopressin release per stimulus pulse was shown to decrease at higher frequencies.[8]

The values of $[DA]_p$ determined from overflow curves are the same at all frequencies tested except 10-Hz, an observation that remains unchanged after administration of drugs which affect $[DA]_p$. The frequency dependence of $[DA]_p$ does not appear to be an effect of interactions with dopaminergic receptors. Haloperidol administration increases $[DA]_p$ by a constant percentage at all frequencies. Similar results are obtained in animals which received chronic administration of haloperidol[47] or l-3,4-dihydroxyphenylalanine (l-DOPA; 250 mg/kg) (data not shown).

In striatal slices, the efficiency of dopamine overflow has also been found to decrease with increasing stimulation frequency,[16,20] and to be greater for single pulses than for pulse trains,[31] an effect that was found to be independent of dopamine autoreceptors. Like $[DA]_p$, the amplitude of the action potential decreases when dopamine neurons fire in bursts.[3,15] This process, termed accommodation, has been documented in several neuronal systems.[27,40] Our analysis of the synaptic overflow curves suggest a similar adaptation in the release process *in vivo*.

Extrapolation to the unstimulated striatum—the basal levels of dopamine in the extracellular fluid

In the unstimulated animal, extrasynaptic concentration gradients are more likely to exist since neurons may fire independently, and the neighboring neurons can take up dopamine which overflows from the synaptic region.[35] The gradients will be quite steep since the values of V_{max} and K_m for uptake allow an estimation of 30 ms as the half-life of dopamine in the extrasynaptic region under unsaturated conditions. However, the kinetic constants obtained from synaptic overflow measurements in the absence of a concentration gradient should allow calculation of the interfacial, extrasynaptic concentration of dopamine in the unstimulated animal. In this calculation, the

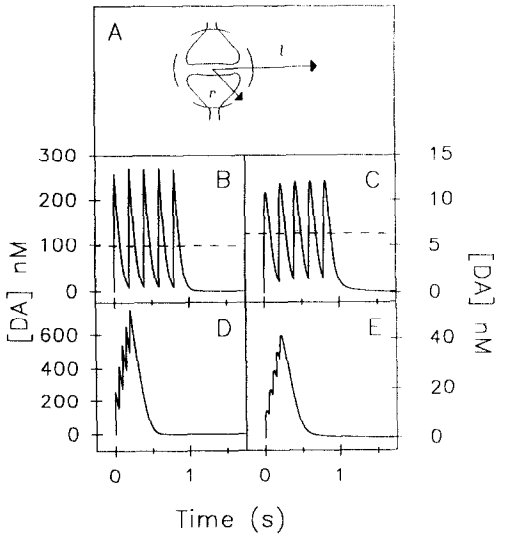

Fig. 7. The extrasynaptic concentration of dopamine calculated for a single neuron firing alone. The concentration of dopamine released is assumed to be pulsatile at the interface of the synapse and the extrasynaptic region, and removed from the extracellular space by uptake sites in the synaptic region governed by Michaelis–Menten kinetics. (A) The synapse is viewed as a spherical concentration source with a radius (r) of 150 nm (Equation 6.60 in Ref. 5); tortuosity and volume fraction[34] were ignored. Firing rate is 5-Hz in the central panels and 20-Hz in the lower panels. (B, D) Concentrations at the interface of the synapse. (C, E) Concentration after diffusion through a solution space (l) of 2 μm. Dashed lines in B and C are the temporally averaged concentrations. Simulation parameters: $[DA]_p = 260$ nM, $V_{max} = 4\,\mu$M/s, $K_m = 0.16\,\mu$M, $D = 6 \times 10^{-6}$ cm^2/s.

value for $[DA]_p$ employed is that found with single pulses or approached with low-frequency stimulations (260 nM), measurements that are closest to the physiological firing rate. The results of such a calculation are shown in Fig. 7 for a single dopamine terminal firing at 5 or 20-Hz, values which are representative of the recorded activity of nigrostriatal neurons during single spike firing and burst firing, respectively.[3]

The interfacial concentration (panel B) decreases rapidly after an impulse at the lower frequency as a result of synaptic uptake, with a time-averaged concentration at the exterior interface of the synapse of 97 nM. Recently an estimate was made of the synaptic concentration of striatal dopamine based on experiments which exploited the competition between binding of [^{3}H]-agonists and the endogenous ligand for the D_2 receptor.[42] The estimated synaptic concentration was approximately 50 nM, in reasonable agreement with our value. However at the higher frequency, the time for uptake between pulses is reduced, and transient, higher concentrations are expected. These calculations are consistent with the results of evoked bursts measured in the rat olfactory tubercle.[13] The right panels of Fig. 7 show that the interfacial concentration can be rapidly diluted by diffusion from the synaptic region. At 5-Hz the concentration becomes quite low with an average concentration during impulse flow of 6 nM at a distance 2 μm from the synaptic interface, a value which is consistent with the spatially and temporally averaged measurements of extracellular dopamine obtained with dialysis.[4,37] Greater extracellular concentrations are found after diffusion from a bursting synapse because the dopamine from successive pulses accumulates in the extracellular space. However, these concentrations may or may not activate receptors; their location with respect to the concentration gradient must play an important role.[36]

CONCLUSIONS

Taken together the results suggest that dopamine in the dorsolateral striatum released by impulse flow primarily acts in a synaptic fashion. Because of the small distance across the synaptic cleft (20 nm), transient intrasynaptic concentrations may exceed the nanomolar range, a concentration that is sufficient to activate both D_1 and D_2 receptors. Recent estimates of the high-affinity state for dopamine binding to receptors in striatal slices give a K_H value of approximately 50 nM, whereas the low-affinity binding state has a value for K_L of greater than 2 μM.[41,42] The extrasynaptic concentration of dopamine at the circumference of the synapse may reach transient concentrations approaching K_H during burst firing, but the concentration will rapidly decrease at distances away from the synapse because of the large concentration gradients generated by the rapid rate of uptake. Because of the high affinity of D_2 receptors, nonsynaptic chemical communication may be possible from this process, but it would appear to be the atypical mode of chemical communication by dopamine in this region. Further speculation requires ultrastructural determination of the relative location of release, uptake, and receptor sites.

Acknowledgements—This research was supported by NSF (BNS 8919705). K.T.K. is a D.O.E. fellow. Helpful discussions with R. N. Adams are gratefully acknowledged.

REFERENCES

1. Amatore C., Kelly R. S., Kristensen E. W., Kuhr W. G. and Wightman R. M. (1986) Effects of restricted diffusion at ultramicroelectrodes in brain tissue. The pool model: theory and experiment for chronomaperometry. *J. Electronanalyt. Chem.* **213,** 31–42.
2. Bracewell R. N. (1986) *The Fourier Transform and Its Applications*, pp. 345–355. McGraw-Hill, New York.
3. Chiodo L. A. (1988) Dopamine-containing neurons in the mammalian central nervous system: electrophysiology and pharmacology. *Neurosci. Biobehav. Rev.* **12,** 49–91.

4. Church W. H., Justice J. B. Jr and Neill D. B. (1987) Detecting behaviorally relevant changes in extracellular dopamine with microdialysis. *Brain Res.* **412,** 397–399.
5. Crank J. (1992) *The Mathematics of Diffusion*, pp. 47–53. Oxford University Press, London.
6. Del Castillo J. and Katz B. (1955) On the localization of acetylcholine receptors. *J. Physiol.* **128,** 157–181.
7. Doucet G., Descares L. and Garcia S. (1986) Quantification of the dopamine innervation in adult rat neostriatum. *Neuroscience* **19,** 427–445.
8. Dutton A. and Dyball R. E. J. (1979) Phasic firing enhances vasopressin release from the rat neurohypophysis. *J. Physiol. Lond.* **290,** 433–440.
9. Eccles J. C. and Jaeger J. C. (1958) The relationship between the mode of operation and the dimensions of the junctional regions at synapses and motor end-organs. *Proc. R. Soc.* **148B** 38–56.
10. Engstrom R. C., Wightman R. M. and Kristensen E. W. (1988) Diffusional distortion in monitoring dynamic events. *Analyt. Chem.* **60,** 652–656.
11. Ewing A. G. and Wightman R. M. (1984) Monitoring the stimulated release of dopamine with *in vivo* voltammetry. II: Clearance of released dopamine from extracellular fluid. *J. Neurochem.* **43,** 570–577.
12. Fowler C. J. and Benedetti M. S. (1983) The metabolism of dopamine by both forms of monoamine oxidase in the rat brain and its inhibition by cimoxaton. *J. Neurochem.* **40,** 1534–1541.
13. Gonon F. G. (1988) Nonlinear relationship between impulse flow and dopamine released by rat midbrain dopaminergic neurons as studied by *in vivo* electrochemistry. *Neuroscience* **24,** 19–28.
14. Gonon F. G. and Buda M. J. (1985) Regulation of dopamine release by impulse flow and by autoreceptors as studied by *in vivo* voltammetry in the rat striatum. *Neuroscience* **14,** 765–774.
15. Grace A. A. and Bunney B. S. (1984) The control of firing patterns in nigral dopamine neurons: burst firing. *J. Neurosci.* **4,** 2877–2890.
16. Hoffmann I. S., Talmaciu R. K. and Cubeddu L. X. (1986) Interaction between edogenous dopamine and dopamine agonists at release modulatory receptors: multiple effects of neuronal uptake inhibitors on transmitter release. *J. Pharmac. Exp. Ther.* **238,** 437–446.
17. Justice J. B. Jr, Nicolaysen L. C. and Michael A. C. (1988) Modelling the dopaminergic nerve terminal. *J. Neurosci. Meth.* **22,** 239–252.
18. Katz B. and Miledi R. (1965) The measurement of synaptic delay and the time course of acetylcholine release at the neuromuscular junction. *Proc. R. Soc.* **161B,** 483–495.
19. Kelly R. and Wightman R. M. (1986) Bevelled carbon-fiber ultramicroelectrodes. *Analyt. chim. acta* **187,** 79–87.
20. Kennedy R. T., Jones S. R. and Wightman R. M. (1992) Dynamic observation of dopamine autoreceptor effects in rat striatal slices. *J. Neurochem.* **59,** 449–455.
21. Kristensen E. W., Bigelow J. C. and Wightman R. M. (1988) Time resolved dopamine overflow from synaptosomes and chopped striatal tissue with rapid superfusion. *Brain Res.* **461,** 44–52.
22. Kristensen E. W., Kuhr W. G. and Wightman R. M. (1987) Temporal characterization of perfluorinated ion exchange coated microvoltammetric electrodes for *in vivo* use. *Analyt. Chem.* **59,** 1752–1757.
23. Kristensen E. W., Wilson R. L. and Wightman R. M. (1986) Dispersion in flow injection analysis measured with microvoltammetric electrodes. *Analyt. Chem.* **54,** 986–988.
24. Kuhr W. G., Ewing A. G., Caudill W. L. and Wightman R. M. (1984) Monitoring the stimulated release of dopamine with *in vivo* voltammetry. I. Characterization of the response observed in the caudate nucleus of the rat. *J. Neurochem.* **43,** 560–569.
25. Kuhr W. G. and Wightman R. M. (1986) Real-time measurement of dopamine release in rat brain. *Brain Res.* **381,** 168–171.
26. Kuhr W. G., Wightman R. M. and Rebec G. V. (1987) Dopaminergic neurons: simultaneous measurements of dopamine release and single-unit activity during stimulation of the medial forebrain bundle. *Brain Res.* **419,** 122–128.
27. Madison D. V. and Nicoll R. A. (1982) Noradrenaline blocks accommodation of pyramidal cell discharge in the hippocampus. *Nature* **297,** 636–638.
28. May L. J., Kuhr W. G. and Wightman R. M. (1988) Differentiation of dopamine overflow and uptake processes in the extracellular fluid of the rat caudate nucleus with fast-scan *in vivo* voltammetry. *J. Neurochem.* **51,** 1060–1069.
29. May L. J. and Wightman R. M. (1989) Heterogeneity of stimulated dopamine overflow within the rat striatum as observed with *in vivo* voltammetry. *Brain Res.* **487,** 311–320.
30. May L. J. and Wightman R. M. (1989) Effects of D-2 antagonists on frequency-dependent stimulated dopamine overflow in nucleus accumbens and caudate-putamen. *J. Neurochem.* **53,** 898–906.
31. Mayer A., Limberger N. and Starke K. (1988) Transmitter release patterns of noradrenergic, dopaminergic and cholinergic axons in rabbit brain slices during short pulse trains, and the operation of presynaptic autoreceptors. *Naunyn-Schmiedebergs. Arch. Pharmac.* **338,** 632–643.
32. Millard J., Stamford J. A., Kruk Z. L. and Whightman R. M. (1985) Electrochemical, pharmacological and electrophysiological evidence of rapid dopamine release and removal in the rat caudate nucleus following electrical stimulation of the medial forebrain bundle. *Eur. J. Pharmac.* **109,** 341–348.
33. Near J. A., Bigelow J. C. and Wightman R. M. (1988) Comparison of uptake of dopamine in rat striatal chopped tissue and synaptosomes. *J. Pharmac. Exp. Ther.* **245,** 921–927.
34. Nicholson C. and Rice M. E. (1990) Diffusion of ions and transmitters in the brain cell microenvironment. In *Volume Transmission in the Brain: Novel Mechanisms for Neuronal Transmission, Vol.* 1 (eds Fuxe K. and Agnati L. F.), pp. 279–294. Raven Press, New York.
35. Nicolaysen L. C., Kieda M., Justice J. B. Jr and Neill D. B. (1988) Dopamine release at behaviorally relevant parameters of nigrostriatal stimulation: effects of current and frequency. *Brain Res.* **460,** 50–59.
36. Pani L., Gessa G. L., Carboni S., Portas C. M. and Rosetti Z. L. (1990) Brain dialysis and dopamine: does the extracellular concentration of dopamine reflect synaptic release? *Eur. J. Pharmac.* **180,** 85–90.
37. Parsons L. H. and Justice J. B. Jr (1992) Extracellular concentration and *in vivo* recovery of dopamine in the nucleus accumbens using microdialysis. *J. Neurochem.* **58,** 212–218.
38. Pickel V. M., Beckley S. C., Joh T. K. and Reis B. J. (1985) Ultrastructural immunocytochemical localization of tyrosine hydroxylase in the neostriatum. *Brain Res.* **225,** 373–385.

39. Press W. H., Flannery B. P., Teukolsky S. A. and Vetterling W. T. (1989) *Numerical Recipes in Pascal*. Cambridge University Press, London.
40. Ranck J. B. (1975) Which elements are excited in electrical stimulation of mammalian central nervous system: a review. *Brain Res.* **98,** 417–440.
41. Richfield E. K., Penney J. B. and Young A. B. (1989) Anatomical and affinity state comparisons between dopamine D_1 and D_2 receptors in the rat central nervous system. *Neuroscience* **30,** 767–777.
42. Ross S. B. (1991) Synaptic concentration of dopamine in the mouse striatum in relationship to the kinetic properties of the dopamine receptors and uptake mechanism. *J. Neurochem.* **56,** 22–29.
43. Scatton B., Dubois A., Dubocovich M. L., Zahniser N. R. and Fage D. (1985) Quantitative autoradiography of ^{3}H-nomifensine binding sites in rat brain. *Life Sci.* **36,** 815–822.
44. Stamford J. A., Kruk Z. L. and Millar J. (1986) *In vivo* voltammetric characterization of low affinity striatal dopamine uptake: drug inhibition profile and relation to dopaminergic innervation density. *Brain Res.* **373,** 85–91.
45. Suaud-Chagny M. F., Mermet C. and Gonon F. (1990) Electrically evoked noradrenaline release in the rat hypothalamic paraventricular nucleus studied by *in vivo* electrochemistry: characterization and facilitation by increasing the stimulation frequency. *Neuroscience* **34,** 411–422.
46. Tassin J. P., Cheramy A., Blanc G., Thierry A. M. and Glowinski J. (1976) Topographical distribution of dopaminergic receptors in the rat striatum. I. Microestimation of [^{3}H]dopamine uptake and dopamine content in microdiscs. *Brain Res.* **107,** 291–301.
47. Wiedemann D. J., Garris P. A., Near J. A. and Wightman R. M. (1992) Effect of chronic haloperidol treatment on stimulated synaptic overflow of dopamine in the rat striatum. *J.Pharmac. exp. Ther.* (in press).
48. Wiedemann D. J., Kawagoe K. T., Kennedy R. T., Ciolkowski E. L. and Wightman R. M. (1991) Strategies fore low detection limit measurements with cyclic voltammetry. *Analyt. Chem.* **63,** 2965–2970.
49. Wightman R. M., Amatore C., Engstrom R. C., Hale P. D., Kristensen E. W., Kuhr W. G. and May L. J. (1988) Real-time characterization of dopamine overflow and uptake in the rat striatum. *Neuroscience* **25,** 513–523.
50. Wightman R. M., Jankowski J. A., Kennedy R. T., Kawagoe K. T., Schroeder T. J., Leszczyszyn D. J., Near J. A., Diliberto E. J. Jr and Viveros O. H. (1991) Temporally resolved catecholamine spikes correspond to single vesicle release from individual chromaffin cells. *Proc. natn. Acad. Sci. U.S.A.* **88,** 10,754–10,758.
51. Wightman R. M. and Zimmerman J. B. (1990) Control of dopamine extracellular concentration in rat striatum by impulse flow and uptake. *Brain Res. Rev.* **15,** 135–144.
52. Williams G. V. and Millar J. (1990) Concentration-dependent actions of stimulated dopamine release on neuronal activity in rat striatum. *Neuroscience* **39,** 1–16.
53. Williams G. V. and Millar J. (1990) Differential actions of endogenous and iontophoretic dopamine in rat striatum. *Eur. J. Neurosci.* **2,** 658–661.
54. Zetterstrom T., Sharp T., Marsen C. A. and Ungerstedt U. (1983) *In vivo* measurement of dopamine and its metabolites by intracerebral dialysis: changes after *d*-amphetamine. *J. Neurochem.* **41,** 1769–1773.

(*Accepted* 1 *June* 1992)

APPENDIX

Overflow curves for dopamine measured in the striatum during stimulated release exhibit a delay between the termination of the stimulation pulses and the maximum dopamine overflow observed. This delay cannot be accounted for by continued firing of dopamine neurons after the stimulation, because unit activity in the substantia nigra decreases below prestimulation values after an electrical pulse train.[26] However, a delay is expected due to diffusion of dopamine from the release site to the electrode.[49] Diffusion in these experiments can occur in three compartments: diffusion through the extracellular fluid,[34] diffusion in the space between the electrode and the tissue,[1] and diffusion through the Nafion coating at the tip of the electrode.[22] Diffusional delays can have a considerable effect on the peak-shaped overflow curves; in addition to the temporal shift of the data, the measured rate of change of dopamine in response to electrical stimulation and the maximal dopamine concentration are decreased from their true values at the synaptic interface of the releasing neurons. In previous work we have grouped all of the diffusion components together and have estimated their joint contribution from the temporal response of the overflow curves.[49]

The temporal distortion caused by diffusion can be removed by deconvolution if the impulse response function of the diffusional barrier is known.[2,39] While the impulse response function of the diffusional components in the extracellular fluid can only be estimated, the response of the Nafion film can be measured *in vitro* by exposure of the electrode to a concentration step of dopamine introduced to the electrode by a flow-injection apparatus.[22] The concentration step is particularly convenient because its derivative directly yields the impulse response function.[10] The response at the inner surface of a film whose outer surface is exposed to a concentration step[5] is:

$$C_0(t)/C_1 = 1 - (4/\pi) \sum_{n=0}^{\infty} [(-1)^n/(2n+1)] \times \exp[-D_m(2n+1)^2\pi^2 t/4l^2] \quad \text{(A.1)}$$

where $C_0(t)$ is the concentration at the inner surface (adjacent to the electrode), C_1 is the dopamine at the film-solution interface, D_m is the diffusion coefficient in the film (1×10^{-9} cm^2/s for dopamine in Nafion,[22] t is the time from the initial exposure, and l is the film thickness. Thus, the temporal response is independent of concentration, but is a function of the film thickness and the diffusion coefficient.[22]

To account for diffusion, the half-rise time of the postcalibration response of the electrodes was used to determine the value of D/l^2 in Equation (A.1) and to calculate the impulse response function of each electrode. While the derivative of the postcalibration response could be used for deconvolution,[10] impulse response functions which contain noise greatly increase artifacts in the data. Deconvolution of the data measured *in vivo* was accomplished by Fourier transformation of the data and impulse response function, division in the Fourier domain, and Fourier transformation of the quotient. This result provides the time-dpendent concentration in the extracellular fluid directly adjacent to the electrode. An example of such a deconvolution is shown in Fig. 1. Notice that the diffusional delay is removed indicating that diffusion in the extracellular fluid plays a minimal role. Oscillations which occur prior to the stimulation and from 4 to 8 s are artefact of the deconvolution procedure.